Recent studies on hohlraum energitics and hohlraum design

Ke Lan, Wenyi Huo, Yongsheng Li, Guoli Ren, Xin Li, Xujun Meng, Changshu Wu, Siyang Zou, Xiumei Qiao, Peijun Gu, Wudi Zheng, Dongxian Lai, and Tinggui Feng

Institute of Applied Physics and Computational Mathematics, P.O. Box 8009-14 Beijing, 100088, People's Republic of China, E-mail: renguoli@hotmail.com

Abstract

In this paper, some recent studies on hohlraum physics at IAPCM (Institute of Applied Physics and Computational Mathematics) were presented, mainly including simulation study on hohlraum physics experiments on SGIII prototype, a novel method for simultaneously determining the maximum radiation temperature and M-band fraction inside a hohlraum, the design of Au + U + Au sandwich hohlraum for 300eV ignition target, and the way to give an initial design of hohlraum size and pertinent drive laser power in order to generate a required radiation profile.

1. Introduction

Hohlraum plays a key role in the study of indirect drive inertial fusion, which converts the shaped laser pulse into a symmetrically time-dependent thermal radiation to assure a nearly isentropic compression of capsule to achieve thermonuclear ignition[1-6]. Hence, worldwide IFE (Inertial Fusion Energy) scientists have been paying much efforts in the study of hohlraum physics[7-11], and a series of theory for hohlraum have been developed, such as the hohlraum coupling efficiency theory, capsule radiation uniformity theory[5], and plasma-filling model[12].

Inertial Fusion program began in China in 1993. We have laser facilities of SGII in Shanghai and SGIII prototype in Mianyang[13-15]. IAPCM in Beijing mainly engages in simulation and theoretical study of Inertial Fusion. The mission of our hohlraum theory group in IAPCM is to study and design the hohlraums for inertial fusion experiments on SG series laser facilities and analyze the experimental results by simulation. The main codes we use for hohlraum physics study are two-dimensional (2-D) radiation hydrodynamic code LARED-H [13,15,16], 1-D multi-group radiation transfer code RDMG[17-19], and 3-D radiation transfer code RT3D[20]. In this paper, we will present some of our studies on hohlraum energitics, hohlraum design and the shock scaling for determing the hohlraum temperature.

In Sec. 2, we will present our simulation study on recent hohlraum physics experiments on SGIII prototype and discuss the laser x-ray coupling efficiency[15]. In Sec. 3, we will present our study on the responses of x-ray ablative shock waves to gold (Au) M-band radiation flux in aluminum (Al) and our novel method for simultaneously determining the maximum radiation temperature and M-band fraction inside a hohlraum by using the shock wave technology[21-22]. In Sec.4, we will present our study on Au + U + Au sandwich hohlraum for 300eV ignition target[23]. In Sec.5, we present our extrapolation of the plasma-filling model to the case of the hohlraums driven by a shaped laser pulse and then present our method of giving an initial design of hohlraum and driven laser to generate a required radiation for 2-D

optimizations[24]. Finally, we summarize in Sec.6.

2. Simulation Study on Recent Hohlraum Experiments on SGIII Prototype

In this section, we use our 2-D code LARED-H to study hohlraum experiments performed on SGIII-prototype laser facility. The SGIII-prototype laser facility consists of eight laser beams with approximately 1 kJ per beam at 0.35 μm. In the experiment, the laser pulse has a 1 ns flat top with 150 ps rising and falling edges, and the eight laser beams simultaneously irradiate the hohlraum from two ends at an incidence cone of 45° angle. We used vacuum Au hohlraums in the experiments. The hohlraum is 1000 μm in diameter and 2100 μm in length, with a 650 μm diameter laser entrance hole (LEH) at each end, denoted as Φ1000 μm × L2100 μm hereafter in this paper. The wall thickness is 25 μm. Here, we only focus on the energetics of this Hohlraum. There are two broad-band soft x-ray spectrometers (SXSs) used for measuring the x-ray flux and spectrum emitted from the hohlraum. One (SXS1) measures from the LEH at an angle of 30° to the hohlraum axis, and the other one (SXS2) measures along the line about 19° from the normal direction of the diagnostic hole. The SXSs are absolutely calibrated 15-channel filtered x-ray diode array that measures x-rays with photon energies ranging from 100 eV to 10 keV.

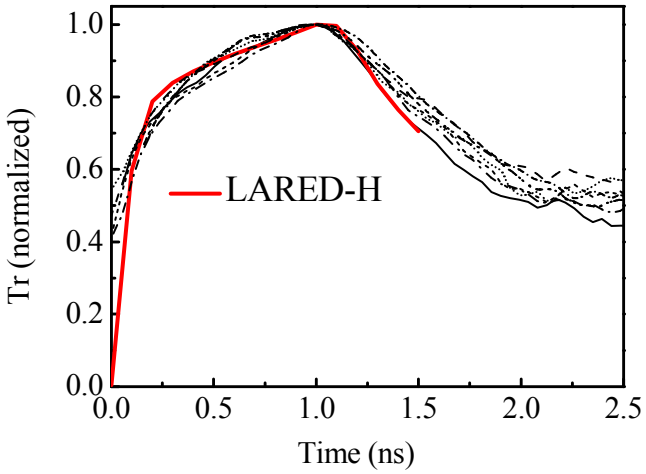

FIG. 1. (Color online) Comparison of the normalized temporal profiles of T_r from the simulation (red line) with those from the observations of SXS1 (black lines).

We firstly compare the simulated radiation and x-ray spectrum with the experimental observations. In our simulations, the radiation and the x-ray spectrum are postprocessed from LARED-H simulation by solving the stationary radiative transport equation. Shown in Figure 1 is a comparison of the peak normalized temporal profiles of T_r from the simulation with those from the observations of SXS1. The laser energies of these shots used in our comparison are around 5 kJ, and the laser energy for simulation is taken as 5 kJ. As shown, the temporal profile of T_r from simulation agrees well with those from observations, except some discrepancies existing on the rising edge. Shown in Fig. 2 is a comparison of the simulated spectrum with the experimental observations from SXS1 in the photon energy

ranging from 100 eV to 5 keV. The Planckian distribution is also presented for comparison. From both simulation and observation, the emissions of N-band and O-band dominate the Hohlraum radiation. Nevertheless, the spectrum depends strongly on the observing direction. In the direction of 30° through LEH, there are three laser spots which can be partially viewed, leading to a higher M-band fraction and a harder spectrum than the Planckian distribution, while in the direction of 19° through the Hohlraum waist, there is no laser spot in the view field and the spectrum is very close to the Planckian distribution.

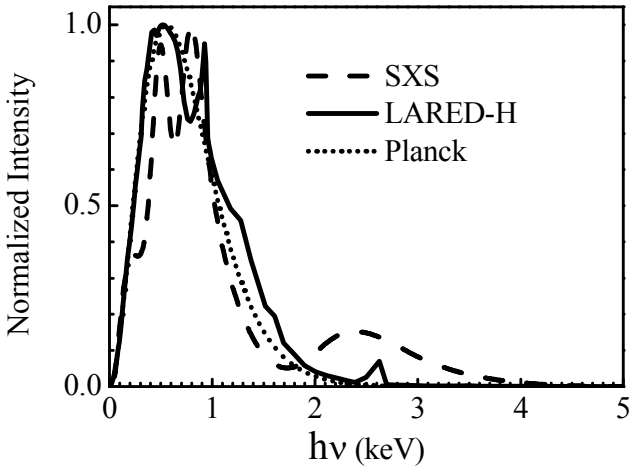

FIG. 2. Normalized spectra of x-ray flux intensity at the maximum radiation measured with SXS1 and postprocessed from LARED-H simulation. The blue dotted line is the Planckian distribution at the corresponding T_r of 200 eV.

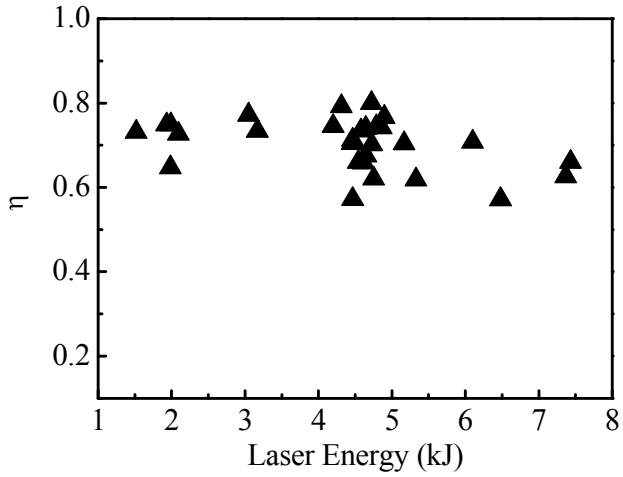

FIG. 3. The coupling efficiencies of hohlraum under different laser energies evaluated from LARED-H simulations.

Now we discuss the coupling efficiency from laser to x-ray. The coupling efficiency from laser to x-ray is defined as a ratio of the emitted x-rays from Hohlraum wall to the input laser energy, and it is usually expressed as $\eta=\eta_a\cdot\eta_x$. Here, η_a is the fraction of laser light absorbed and η_x is the laser to x-ray conversion efficiency. In simulation study, η_x can be

obtained from the simulations, while η_a is related to the laser-plasma interactions measured by the experiments. We calculate the coupling efficiency by adjusting the laser energy so that the calculated peak radiation temperature equals to the measured peak radiation temperature. Figure 3 shows the coupling efficiency for all shots. As a result, the coupling efficiency is around 70% for Φ1000 μm ×L2100 μm hohlraums driven by a 1 ns flap top laser pulse. According to the simulations from LARED-H, the conversion efficiency from laser to x-ray for this kind of Hohlraum is relatively high, around 85%. Hence, the average coupling efficiency of 70% corresponds to a backscatter of about 15%. Notice that the discrepancy of data shown in Figure 3 is somewhat large, which may be due to the fact that we do not use the beam smoothing technology on SGIII-prototype, and thus it leads to an unstable backscatter refraction produced by the laser plasma interactions.

3. Novel Method for Determining the M-Band Fraction in A Hohlraum

In this section, we present our novel method for determining f_m by using the shock wave measurement technique. Here, f_m is the M-band fraction in total x-ray flux inside hohlraum. The code used for this study is RDMG.

The 2–4 keV Au M-band radiation emitted from hohlraum wall is an important issue in the indirect-drive Inertial Fusion research[1,4,5,25]. Generally, SXS is used to measure the x-ray flux streaming out of the hohlraums along a line through LEH and the M-band fraction can be deduced from the spectrum. However, it is difficult for SXS to obtain the real M-band fraction inside a hohlraum because of the following reasons. Firstly, the radiation flux measured by SXS is often influenced by the cold plasmas outside the hohlraum and the shrinking effect of the LEH. Secondly, the measured flux of SXS strongly depends on the direction of observation. Therefore, it is necessary to develop a complementary measurement technique so that one can determine the M-band fraction in different ways to check and evaluate the simulations, especially when there are discrepancies between the SXS observations and numerical simulations[15,26].

The shock wave technique is widely used in hohlraum experiments to determine the peak T_r inside a hohlraum[21,27-29]. By measuring the shock wave velocity V_s in a witness plate mounted on the hohlraum wall, T_r can be determined via a scaling relation of T_r with V_s. Generally, the shock scaling is obtained from the simulations by using a radiation source of Planckian spectrum. However, the M-band radiation can not be ignored and the radiation is far from Planckian distribution inside a hot hohlraum, especially in a Au hohlraum. In fact, V_s depends on the ablation pressure which is related to the albedo of witness material, while the albedo is related to the material opacity. As a result, V_s should be related to the spectrum of a radiation source and the material opacity. It is therefore possible to determining f_m by using this character of the shock wave.

Shown in Figure 4 are variations of opacity with frequency in Al (Z=13) and Ti (Z=22), which are quite different from each other. For Al, the opacity is low in the region of O-band (~ 450 eV, mainly referring to the radiations related to n=5 of Au) and N-band (~ 800 eV, related to n=4 of Au) but high in M-band region (2–4 keV, related to n=3 of Au). It means that there are strong absorptions in M-band for Al. However, for Ti, the strong absorptions appear in the region of O-band and N-band. According to this characteristic, we predict that

the influence of the M-band fraction on the shock wave behaviors should be different in Al and Ti.

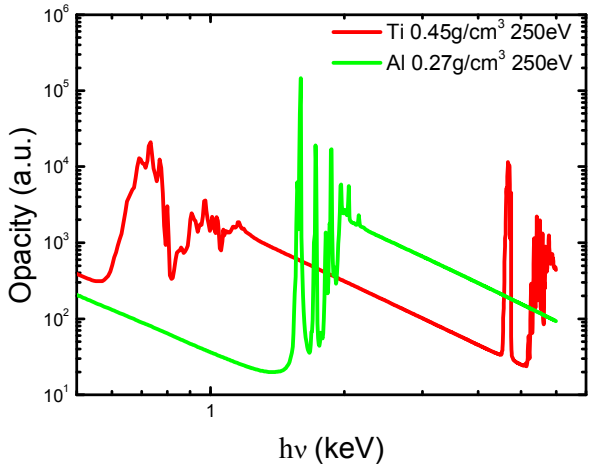

FIG. 4. (Color online) Opacity vs frequency for Al and Ti.

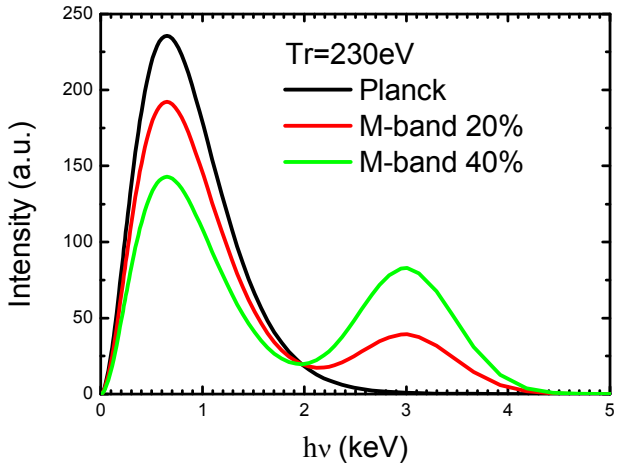

FIG. 5. (Color online) Spectral distributions of radiation source for simulation.

We modeled the ablation processes in Al and Ti plates driven by an x-ray source obtained from LARED-H (shown in Figure 1) with spectrum distribution in Figure 5. By varying the M-band fraction in the sources, we obtain the relations of V_s with f_m for Al and Ti in the range of 200 to 300 eV. As a result, V_s decreases with f_m in Al at a given radiation temperature, while it increases in Ti. It confirms our previous prediction that the M-band fraction has much different influence on the shock wave velocity in Al and Ti. Thus, the radiation temperature T_r cannot be uniquely determined by the shock wave velocity in Al plate if the M-band fraction f_m inside a hohlraum is obviously higher than that in the Planckian spectrum.

Nevertheless, we can determine T_r and f_m in a hohlraum simultaneously if both shock velocities in Al and Ti samples are known in one experimental shot. Here, we give an example. Figure 6 gives contour lines of the shock velocities in Al and Ti in f_m / T_r plane,

calculated from above shock scaling. If the measured V_s is 5.5×10^6 cm/s in Al and 3.3×10^6 cm/s in Ti, then the cross of these two contour lines gives T_r =215 eV and f_m =20%. The precision of this method depends on the errors of simulation and shock wave velocity measurement. The simulation error is mainly caused by the uncertainty of opacity. According to our simulations, an error of 10% in opacity leads to 1% error in shock wave velocity for Al and 1.3% for Ti. The measurement error of shock wave velocity is typically 1%–2%. As shown in Figure 6, it gives $T_r = 215 \pm 3$ eV and $f_m = 20 \pm 5\%$ after taking the measurement error of 2% into consideration. In fact, it is possible to improve the precision of our method if three kinds of witness plates are used.

It should be pointed out that a serious preheat may lead to an obvious expansion and rarefaction of the rear surface of Ti, resulting in an remarkable delay of the shock unloading time and thus causing a big error in calculating the experimental shock velocity. Nevertheless, it can be skillfully avoided if we choose to compare the simulations with the measured shock unloading time differences, instead of the shock velocities.

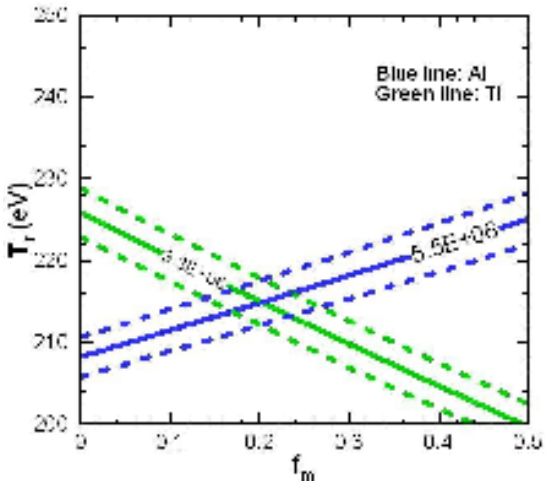

FIGURE 6. (Color online) The errors of T_r and f_m induced by 2% uncertainties of shock wave velocity measurement.

4. Study on Au + U + Au Sandwich Hohlraum for 300ev Ignition Target

In ignition targets designs, U or U based cocktail hohlraums are usually used because the Rosseland mean opacity of U is higher than that of Au at the radiation temperature for ignition. However, it should be noticed that there is a longer than 10 ns prepulse at temperatures lower than 170 eV in the radiation drive for ignition, while the opacity of U is actually lower than that of Au within this low temperature region. In addition, the depth penetrated by radiation is only several micrometers under a 300eV radiation. We therefore proposed an Au + U + Au sandwich hohlraum for ignition targets in this work. The code we used for this study is RDMG, and the absorption cross section is calculated with our relativistic Hartree-Fock-Slater (HFS) self-consistent average atom model OPINCH[30].

Firstly, we use RDMG to simulate the radiation ablation of U-Au mixture planar targets, which are exposed to a 1 ns radiation source $T_0 t^{0.18}$. Here, T_0 is radiation temperature

at 1ns and t is time. The target thickness is taken as 25 μm. At T_0 = 300 eV, the minimum energy absorption is produced in the mixture of 25% Au + 75% U, and it is around 80% relative to pure Au. The energy absorption of pure U relative to that of pure Au is about 85%. Nevertheless, when the temperature drops in the range of approximately 40 eV to 170 eV, at densities concerned for radiation ablation in inertial fusion energy study, such as 1 g/cm^3, the opacity of Au is higher than that of U, according to OPINCH. In this temperature range, the bound electrons in the principal quantum number n=4 of Au is partially ionized, but there is still much bound electrons in this shell; while for U, n=4 is almost fully occupied. In Figure 7, we give the ratio of energy absorptions (U-Au mixture over pure Au) under radiation drive of T_0=110 eV. As shown, the energy absorption of pure U relative to that of pure Au is near 140%. Approximately, the mixture of 75% Au and 25% U has the minimum energy absorption at 110 eV, but with weak superiority compared to pure Au. The albedo of U-Au mixture is also presented in the figure. As shown, the albedo of pure U is obviously smaller than that of pure Au at 110 eV.

On the other hand, our simulation showed that most of the radiation energy is absorbed only within a thin and diffusively heated layer of the hohlraum interior surface. Under a typical radiation drive source in ICF study, such as 300 eV, the Marshak wave[31] front is steep and the temperature maintains a flat profile only within a penetration depth of several micrometers, and then it drops sharply to cold material temperature. Hence, a whole cocktail hohlraum is actually not necessary for ignition target.

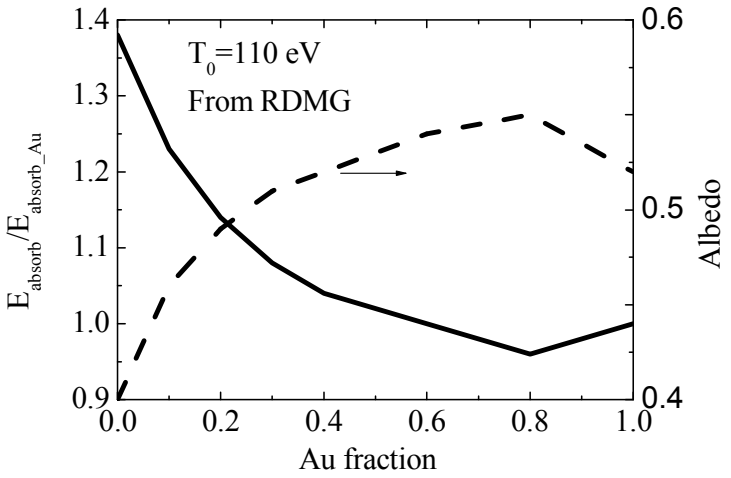

FIG. 7. Ratios of albedo (dashed line) and energy absorption (solid line) in U-Au mixture to those in pure Au at T_0=110eV.

Considering all results given above, we therefore propose a Au + U + Au sandwich hohlraum for the ignition target. The schematic of sandwich wall is shown in Figure 8. The purpose of using a Au layer in the interior surface of hohlraum is, in addition to preventing the U from oxidizing, to increase the albedo during prepulse, recalling Au has a higher opacity than U at low temperature range. It is good to increase albedo for improving the capsule radiation uniformity during the prepulse.

We use RDMG simulation results to give the sandwich design for a typical National Ignition Facility (NIF) radiation drive[32,33]. The target thickness is taken as 25 μm. From

simulation results, the energy absorption of an Au + U target reaches its minimum when the inner Au layer is around 0.1 mm, but nevertheless its variation is small when the inner Au layer is within 0.6 mm. When the inner Au layer is thicker than 0.6 mm, the energy absorption increases seriously. Taking the inner Au layer as 0.1 mm, we further choose the optimum thickness of the medium U layer by simulation. In Figure 9, the energy absorption of an Au + U + Au sandwich relative to a pure U target as a function of U layer thickness is presented. As shown, the optimum thickness of U layer is around 5 μm.

The advantage of a sandwich target is almost the same as that of a cocktail target in saving wall loss, while the former design not only remarkably simplifies the target fabrication and uses less depleted U material, but also increases the albedo during prepulse, which is good for reducing the hot-spot to wall emission ratio and improving the initial capsule radiation uniformity. Wilkens[34] *et al.* (2007) reported on the fabrication techniques for a gold cocktail hohlraum which has the similar structure as our sandwich hohlraum except with a cocktail medium layer, and more, `they used it mainly for technical purposes.

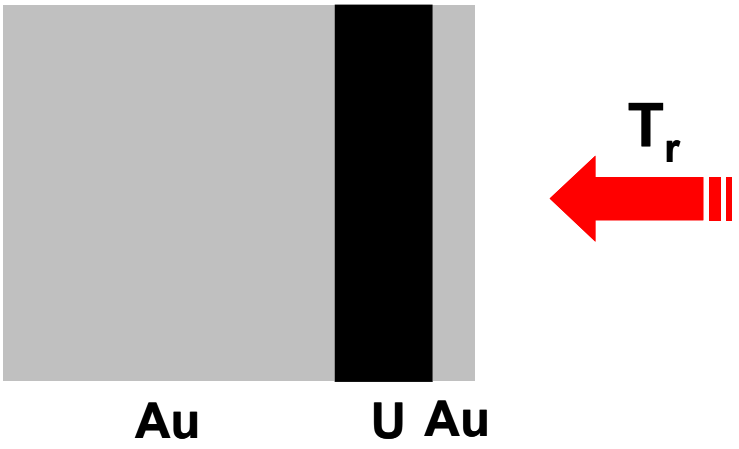

FIG. 8. Schematic of the Au + U + Au sandwich target in ignition target design.

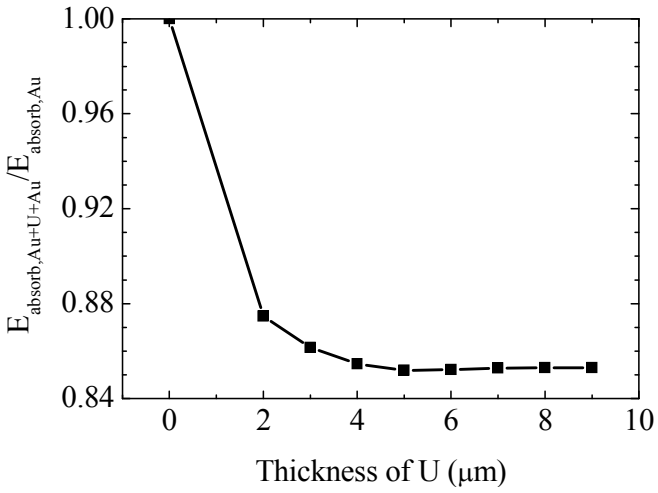

FIG. 9. The energy absorption of a Au + U + Au target relative to a pure Au target as a function of the U thickness. The interior Au layer facing to the radiation source is taken as 0.1 μm .

5. Initial Design For Generating A Required Shaped Radiation Pulse

In the indirect drive inertial fusion study, it needs to design a hohlraum and pertinent drive laser pulse to produce a required time-dependent radiation to assure a nearly isentropic compression of capsule inside the hohlraum to achieve thermonuclear ignition. Usually, the optimal design is finished with 2-D simulations. However, what are the initial values of hohlraum size and laser pulse that we should put into 2-D simulation for further optimization? As known, the optimization searching process may be extremely laborious and computationally expensive if without a suitable initial value. In this section, we present our method of giving an initial design of hohlraum size and pertinent laser drive for producing a required shaped radiation inside a hohlraum.

The plasma-filling model[7,12,35] was developed for hohlraum driven by laser with a constant power. Now we extend it to case when a hohlraum is driven by a shaped laser pulse with high contrast (>1) between different steps, which is a typical drive for ignition goal. The maximum radiation temperature is produced in the last step of laser pulse. It is assumed that the differences of T_r between steps are large and the mass of wall material ablated in each step of radiation is much larger than that in its former step. Thus, the mass of wall ablated in each step can be calculated independently. Nevertheless, the ablation in each step increases the wall albedo and contributes to the sum of the ablated mass, and eventually influences the plasma-filling time in the hohlraum.

Assuming that the laser pulse has J steps, we use P_j to denote the incident laser power, τ_j the time width, $T_{r,j}$ the radiation temperature, $T_{r,j} \propto (t-\sum_{j'=1}^{j-1}\tau_{j'})^{k_j}$, and α_j the wall albedo of the jth step ($j=1, \cdots, J$). Here, k_j is a fitted coefficient describing the time variation of radiation temperature in jth step. The coupling efficiency η from laser to x-ray is assumed to be the same for all steps, and the power balance for the jth step is $\eta P_j = \sigma T_{r,j}^{\ 4}\{(1-\alpha_j)A_W + A_H\}$. Here, A_W is hohlraum wall area, A_H is area of LEH, and σ is the Stefan-Boltzmann constant. We express α_j as $1-H_j/(T_{r,j}^{\gamma_j}\tau_j^{\beta_j})$, where H_j, γ_j and β_j are fitted coefficients. We can approximately relate $T_{r,j}$ to P_j and τ_j by defining a hohlraum geometrical factor $f_{H,j}=1+A_H/[(1-\tilde{\alpha}_j)A_W]$, where $\tilde{\alpha}_j$ is an average albedo of the jth step. Inserting above expressions of α_j and $f_{H,j}$ into the power balance, we have $T_{r,j}=D_j P_j^{E_j}\tau_j^{F_j}$, in which $D_j=\eta\left(H_j f_{H,j}\sigma A_W\right)^{-1}$, $E_j=1/(4-\gamma_j)$ and $F_j=\beta_j/(4-\gamma_j)$. We denote the wall ablated mass in the j th step of radiation as m_j, then the total ablated mass is $\sum_{j=1}^{J} m_j$ and the material density in hohlraum is $\rho = S_{abl}/V_{hohl}\times\sum_{j=1}^{J} m_j$. Here, S_{abl} is the effective area of wall being ablated and V_{hohl} is hohlraum volume.

We neglect the index J for the last step in which the maximum temperature in hohlraum is created. Considering a Au hohlraum driven by a 3ω shaped laser pulse, we have the ion density in unit of the critical density $n_i = 0.339 \times S_{abl} / V_{hohl} \sum_{j=1}^{J} m_j$. Using the power balance in the laser hot channel and pressure balance between the laser channel and surrounding plasma, we obtain $P\,(\mathrm{TW}) = 3.1\times10^{-16} \times n_i^{4.6} n_e^{-6.6} (T_r / eV)^{6.67} (1-n_e)^{0.5}$. Putting the expression of the ablated mass[4] and $T_r = DP^E \tau^F$ into P(TW) and solving for n_e, we obtain electron density in the last laser step:

$$n_e \left(1-n_e\right)^{-\frac{1}{13.2}} = 4.47\times10^{-3} \times D^{1.01} \times P^{1.01E-\frac{1}{6.6}} \tau^{1.01F} n_i^{0.697}$$

Because n_e depends on driven laser pulse, wall material and hohlraum size, so the plasma-filling model can be used in the initial design of a hohlraum target and pertinent laser.

Nevertheless, a criterion is needed for designing a suitable hohlraum. When the plasma filling becomes serious, the laser absorption region shifts far from the hohlraum wall, and more, the hydrodynamic loss and the thin coronal radiative loss from LEH increase rapidly. Considering the driven laser is decayed mainly via inverse bremsstrahlung absorption inside hohlraum, we can define a hohlraum inverse bremsstrahlung absorption number as $n_{IB}=R_{LEH}/\lambda_{IB}\sin\theta$, where R_{LEH} is the LEH radius, λ_{IB} is the inverse bremsstrahlung absorption length, and θ is the incident angle of laser. According to our experiences in successfully designing the hohlraums for experiments on SG laser facilities and ignition targets, a useful semi-empirical criterion is n_{IB}=1. More, we take θ=45° for hohlraums designed for SG series and θ=50° for ignition hohlraums.

This method has been used successfully to give initial designs to produce the required radiation profiles on SGIII prototype, the 300eV radiation drive for Au hohlraum[2], and the 300eV radiation drive for NIF[32,33].

6. Summary

We have presented some of our recent studies on hohlraum physics. Firstly, the simulation results of hohlraum radiation from our 2-D code LARED-H agree with the observations from SXS at different view angles on SGIII laser facility, and the coupling efficiency from laser to x-ray is around 70%. Secondly, we had proposed a novel method for simultaneously determining the maximum radiation temperature and M-band fraction inside a hohlraum by using the shock wave technology. The precision of this method depends on the errors of simulation and shock wave velocity measurement. Thirdly, we had proposed a 0.1 μm Au + 5 μm U + 19.9 μm Au sandwich hohlraum for 300eV ignition target. Finally, we had extrapolated the plasma-filling model to the case of the hohlraums driven by a shaped laser pulse, and then applied it to initial design of a hohlraum and pertinent drive laser in order to generate a required radiation.

Acknowledgements

This work was performed under National Basic Research Program of China (973 program, No. 2007CB814800).

REFERENCES

[1] ATZENI, S. & MEYER-TER-VEHN J. The Physics of Inertial Fusion. Oxford Science Press, London (2004).

[2] Haan, Steven W., et al., "Design and modeling of ignition targets for the National Ignition Facility", Phys. Plasmas **2** (1995) 2480-2487

[3] HOFFMANN, D.H.H., "Intense laser and particle beams interaction physics toward inertial fusion", *Laser Part. Beams* **26** (2008) 295–296.

[4] LINDL, J. D., "Development of the indirect-drive approach to inertial confinement fusion and the target physics basis for ignition and gain", *Phys. Plasmas* **2** (1995) 3933.

[5] LINDL, J.D., et al., "The physics basis for ignition using indirect-drive targets on the National Ignition Facility", *Phys.Plasmas* **11** (2004) 339–491.

[6] RAMIS, R., RAMIREZ,J.&SCHURTZ, G., "Implosion symmetry of laser-irradiated cylindrical targets", *Laser Part. Beams* **26** (2008) 113-126.

[7] DEWALD, E.L., et al., "Radiation-driven hydrodynamics of high-Z hohlraums on the national ignition facility", *Phys. Rev. Lett.* **95** (2005) 215004.

[8] JONES, et al., "Proof of principle experiments that demonstrate utility of cocktail hohlraums for indirect drive ignition", *Phys. Plasmas* **14** (2007) 056311.

[9] ORZECHOWSKI, T.J., et al., "The Rosseland mean opacity of a mixture of gold and gadolinium at high temperatures", *Phys. Rev. Lett.* **77** (1996) 3545–3548.

[10] SIGEL, R., et al., "X-ray generation in a cavity heated by 1.3 or 0.44 mm laser light III Comparison of the experimental results with theoretical predictions for x-ray confinement", *Phys. Rev. A* **38** (1988) 5779-5785.

[11] SUTER, L. J., et al., "Radiation drive in laser-heated hohlraums", *Phys. Plasmas* **3**, (1996) 2057–2062.

[12] SCHNEIDER, M.B., et al., "Plasma filling in reduced-scale hohlraums irradiated with multiple beam cones", *Phys. Plasmas* **13** (2006) 112701.

[13] CHANG, T., et al., "Laser hohlraum coupling efficiency on the Shenguang II facility", *Phys. Plasmas* **9** (2002) 4744-4748.

[14] X. T. He and W. Y. Zhang, "Inertial fusion research in China", The European Physical Journal D **44** (2007) 227-231.

[15] HUO, W., et al., "Simulation study of hohlraum experiments on SGIII-prototype laser facility", *Phys. Plasmas* **17** (2010) 123114.

[16] DUAN, Q., et al., "Two-dimensional numerical simulation of laser 2irradiated gold disk targets", *Chinese Jour. of Comp. Physics* **19** (2002) 57 -61.

[17] FENG, T.G., LAI, D.X. & XU, Y., "An artificial-scattering iteration method for calculating multi-group radiation transfer problem", *Chinese J. Comput. Phys.* **16** (1999) 199–205.

[18] GU, P., PEI, et al., “Investigation on on-LTE radiation emitted from a laser-irradiated Au disk”, *Science in China Ser. G Physics, Mechanics and Astronomy* **48** (2005) 1-16.
[19] XU, Y., et al., “A clean radiation environment for opacity measurements of radiatively heated material”, *Phys. Plasmas* **14** (2007) 052701.
[20] FENG, T. & LAI, D., “Semi-random simulation method for calculating 3-D radiation transfer problems in cavity”, *Science in China (Series E)* **39** (1996) 461.
[21] LI, Y., et al., “Radiation-temperature shock scaling of 1 ns laser-driven hohlraums”, *Phys. Plasmas* **17** (2010b) 042704.
[22] LI, Y., HUO, W. &LAN, K., “A novel method for determining the *M*-band fraction in laser-driven gold hohlraums“*Phys. Plasmas* **18** (2011) 022701.
[23] LI, X., LAN, et al., “Study on Au + U + Au sandwich hohlraum wall for ignition targets”, *Laser Part. Beams* **28** (2010a) 75-81.
[24] LAN, K., et al., “An initial design of hohlraum driven by a shaped laser pulse”, *Laser Part. Beams* **28** (2010) 421-427.
[25] OLSON, et al., “Preheat effects on shock propagation in indirect-drive inertial confinement fusion ablator materials”, J. A., *Phys. Rev. Lett.* **91** (2003) 235002.
[26] ROBEY, et al., “Experimental measurement of Au *M*-band flux in indirectly driven double-shell implosions”, *Phys. Plasmas* **12** (2005) 072701.
[27] KAUFFMAN, et al., “High temperatures in inertial confinement fusion radiation cavities heated with 0.35 μm light. ”, *Phys. Rev. Lett.* **73** (1994) 2320.
[28] HATCHETT, S. P. “Ablation Gas Dynamics of Low-Z Materials Illuminated by Soft X-Rays”, LLNL, Livermore(1991).
[29] REMINGTON, et al., “Single-mode and multimode Rayleigh-Taylor experiments on NOVA”, *Phys. Plasmas* **2** (1995). 241.
[30] SERDUKE, et al., “WorkOp-IV summary: lessons from iron opacities”, J. Quant. Spectro. & Rad. Trans. **65** (2000) 527–541.
[31] MARSHAK, R.E., “Effect of radiation on shock wave behavior”, Phys. Fluids **1**(1958) 24–29.
[32] HAMMER, J.H. & ROSEN, M.D., “A consistent approach to solving the radiation diffusion equation”, Phys. Plasmas 10 (2003) 1829–1845.
[33] GLENZER, et al., “Experiments and multiscale simulations of laser propagation through ignition-scale plasmas”, Nat. Phys. 3 (2007) 716–719.
[34] WILKENS, et al., “Developing depleted uranium and gold cocktail hohlraums for the National Ignition Facility”, Phys. Plasmas 14 (2007) 056310.
[35] MCDONALD, J.W., et al., “Hard x-ray and hot electron environment in vacuum hohlraums at the National Ignition Facility”, *Phys. Plasmas* **13** (2006) 032703.